Available online at www.sciencedirect.com
SCIENCE DIRECT®
Journal of Sound and Vibration 271 (2004) 25–45
JOURNAL OF SOUND AND VIBRATION
www.elsevier.com/locate/jsvi

Axisymmetric vibration and damping analysis of rotating annular plates with constrained damping layer treatments

Horng-Jou Wang, Lien-Wen Chen*

Department of Mechanical Engineering, National Cheng Kung University, Tainan 70101, Taiwan, ROC

Received 13 May 2002; accepted 4 March 2003

Abstract

The axisymmetric vibration and damping of rotating annular plates with constrained damping layer treatments are analyzed in the present paper. The discrete layer annular finite element method is employed to derive the equations of motion for the rotating composite plate where the geometry stiffness matrix induced by rotation is evaluated from solutions of static problems. The viscoelastic material in the central layer is assumed to be incompressible, and the extensional and shear moduli are described by complex quantities. Complex-eigenvalued problems are then solved, and the frequencies and modal loss factors of the composite plate are extracted. The effects of stiffness and thickness of the viscoelastic and constraining layers on the natural frequencies and modal loss factors of rotating composite plates are presented. Also, the composite plates with various boundary conditions and partial treatments are discussed.

1. Introduction

The plate with the constrained damping layer treatment is well known to have high damping capacity and high resistance to resonant noise and vibration. Numerous investigations on the vibration and damping properties of basic structures, such as beams and rectangular plates, with constrained damping layer treatments are available. Kerwin [1] discussed the problem first. Ross et al. [2] presented a fourth order theory to predict damping in plates with constrained layer treatments. DiTaranto [3] derived a sixth order theory for constrained layer damped beams with arbitrary boundary conditions. The governing equations of flexural vibration of a symmetrical sandwich rectangular plate were presented by Mead [4]. Rao and Nakra [5] proposed a set of twelfth order partial differential governing equations including bending–extension coupling of

*Corresponding author. Tel.: +886-6-2757575 ext. 62143; fax: +886-6-2352973.
E-mail address: chenlw@mail.ncku.edu.tw (L.-W. Chen).

0022-460X/03/$ - see front matter
doi:10.1016/S0022-460X(03)00260-8

unsymmetrical sandwich plates. Rikards et al. [6] studied the vibration and damping of laminated composite beam by using a simple Timoshenko beam finite element. Cupial and Niziol [7] considered a three-layered rectangular plate with a viscoelastic core layer and two laminated face layers by the first order shear deformation theory. Zapfe and Lesieutre [8] investigated the dynamic behavior of composite sandwich beams with integral damping layers by discrete layer beam finite elements.

Circular plates are widely used in mechanical applications, and vibrations of annular plates have also been discussed for many decades. For example, Rao and Prasad [9], Irie et al. [10], and Wang et al. [11] discussed the vibration of isotropic stationary annular plates, and Kirkhope and Wilson [12], Nigh and Olson [13], and Liu et al. [14] studied the cases of rotating plates. However, the studies of constrained damping layer treatment to annular plates were limited. Roy and Ganesan [15] developed a finite element method for vibration and damping analyses of circular plates with the constrained damping layer treatment. Yu and Huang [16] derived the equations of motion of a three-layer circular plate based on the thin shell theory to handle the very thin viscoelastic core layer problem. In both mentioned papers, the stationary plates with fully constrained damping layer treatment and the solutions of iso-symmetric annular plate were considered. Seubert et al. [17] investigated rotating disks with fully constrained damping layer by using the commercial finite element analysis program and measurements.

In practical applications, partial damping treatment is necessary because of material, thermal, packaging, weight or cost constraints. In the present paper, the axisymmetric vibration and damping characteristics of rotating annular plates with constrained damping layer treatment will be studied. In order to discuss cases of partially treatments and various boundary conditions conveniently, the discrete layer annular finite element method is developed to derive the equations of motion of the rotating composite plate system. The initial stresses induced by the centrifugal force are calculated from the solutions of static problems and are taken into account in the strain energy expression to obtain the geometric stiffness matrix that increases the plate stiffness. By using the complex modulus representations of viscoelastic material, substituting desired material properties into the corresponding layers, and assembling all elements in various ways, the complex eigenvalue problems are obtained and then natural frequencies and modal loss factors of rotating annular plates with various type of treatments and boundary conditions can be solved. The effects of many design parameters of the rotating damped annular plate are discussed.

2. Finite element formulation

As shown in Fig. 1, the annular plate of inner radius a and outer radius b is partially treated with a constrained damping layer and rotates about z-axis at a constant angular speed Ω. The annular constrained damping layer covering has an inner radius a' and outer radius b' and is composed of two layers. The upper layer (designated as layer 3) is a pure elastic, isotropic and homogeneous constraining layer and the middle layer (layer 2) is the linear viscoelastic material layer. Layer 2 is capable of adhesively dissipating vibratory motions. The host annular plate is assumed to be undamped, isotropic and homogeneous and is designated as layer 1. The thicknesses of three layers are h_1, h_2, and h_3, respectively. And the interfaces between layers are assumed to be perfectly bonding.

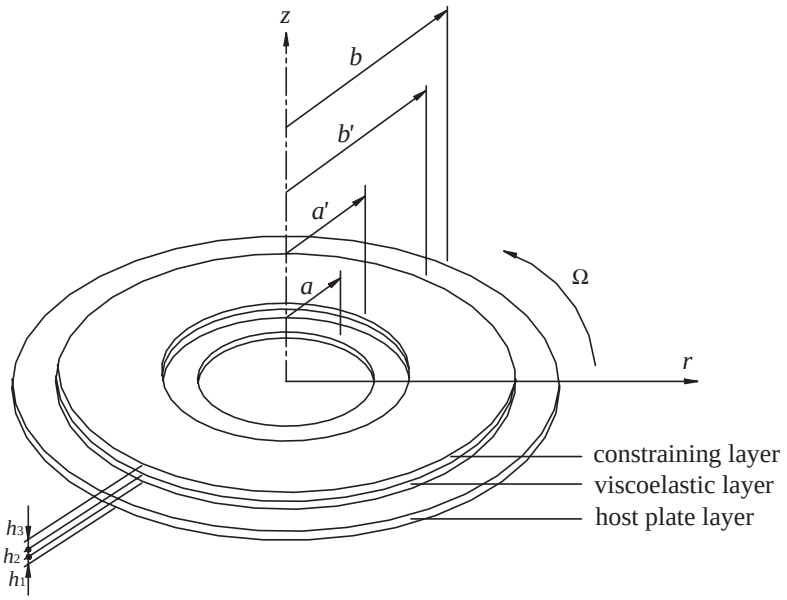

Fig. 1. The rotating annular plate with partially constrained damping layer treatment.

In order to consider the composite plate with various types of treatments and boundary conditions conveniently, the discrete layer annular finite element method is developed to derive the equations of motion for the rotating composite plate system. The discrete layer annular finite element adopted is shown in Fig. 2(a). The axisymmetric annular finite element of inner radius r_i and outer radius r_o for layer i has eight-degree-of-freedom. These are the displacements in the $r$direction— U_i^A, U_{i+1}^A, U_i^B and U_{i+1}^B, the transverse displacements— W^A and W^B, and the rotation angles—Θ^A and Θ^B. Under the assumption that the transverses displacements are constant through the thickness of the plate, the nodal degrees of freedom for three-layered discrete layer annular finite elements are shown in Fig. 2(b).

The displacement field of layer i, $\boldsymbol{u}_i = \{u_i \quad w_i\}^{\mathrm{T}}$, can be expressed in terms of the in-plane displacements of the adjacent layer interfaces and the transverse displacement, $\{U_i U_{i+1} W\}^{\mathrm{T}}$, as

$$\begin{Bmatrix} u_i(r,z,t) \\ w_i(r,t) \end{Bmatrix} = \boldsymbol{L}_{1,i}(z) \begin{Bmatrix} U_i(r,t) \\ U_{i+1}(r,t) \\ W(r,t) \end{Bmatrix}, \tag{1}$$

where $\boldsymbol{L}_{1+i}$ is the transverse thickness interpolation matrix for layer i and is shown as below

$$\boldsymbol{L}_{1,i}(z) = \begin{bmatrix} \left(\frac{1}{2} - \frac{z}{h_i}\right) & \left(\frac{1}{2} + \frac{z}{h_i}\right) & 0 \\ 0 & 0 & 1 \end{bmatrix}. \tag{2}$$

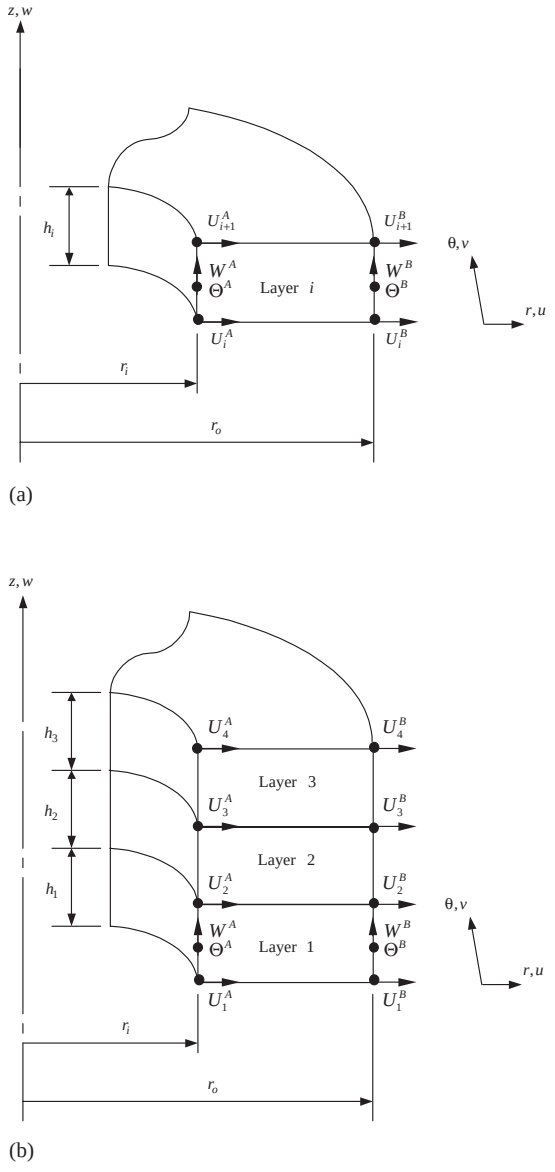

Fig. 2. The axisymmetric discrete layer annular finite element: (a) basic element; (b) three-layered element.

Using a further interpolation in the r direction, the displacements of the two layer interfaces can be expressed in terms of the nodal degrees of freedom

$$\begin{Bmatrix} U_i(r,t) \\ U_{i+1}(r,t) \\ W(r,t) \end{Bmatrix} = \boldsymbol{L}_2(r)\boldsymbol{U}_i^e(t), \tag{3}$$

where $\boldsymbol{L}_2$, the interpolation matrix and $\boldsymbol{U}_i^e$, the vector of nodal displacements of the element, are given by

$$\boldsymbol{L}_2(r) = \begin{bmatrix} n_u^A & 0 & 0 & 0 & n_u^B & 0 & 0 & 0 \\ 0 & n_u^A & 0 & 0 & 0 & n_u^B & 0 & 0 \\ 0 & 0 & n_w^A & n_\Theta^A & 0 & 0 & n_w^B & n_\Theta^B \end{bmatrix}, \tag{4}$$

$$\boldsymbol{U}_i^e = \left\{ U_i^A \quad U_{i+1}^A \quad W^A \quad \Theta^A \quad U_i^B \quad U_{i+1}^B \quad W^B \quad \Theta^B \right\}^{\mathrm{T}}, \tag{5}$$

$$n_u^A = (1-\xi), \quad n_u^B = \xi, \quad n_w^A = (1 - 3\xi^2 + 2\xi^3), \quad n_w^B = (3\xi^2 - 2\xi^3), \tag{6a-d}$$

$$n_\Theta^A = (\xi - 2\xi^2 + \xi^3), \quad n_\Theta^B = (-\xi^2 + \xi^3), \quad \xi = \frac{r - r_i}{r_o - r_i}. \tag{6e-g}$$

The linear strains in layer i of the annular plate can be written in terms of the displacement

$$\varepsilon_i = \mathscr{D}\boldsymbol{u}_i, \tag{7}$$

where the strain vector $\varepsilon_i = \left\{ \varepsilon_{r,i} \quad \varepsilon_{\theta,i} \quad \gamma_{rz,i} \right\}^{\mathrm{T}}$ and $\mathscr{D}$ is the differential operator matrix

$$\mathscr{D} = \begin{bmatrix} \dfrac{\partial}{\partial r} & 0 \\ \dfrac{1}{r} & 0 \\ \dfrac{\partial}{\partial z} & \dfrac{\partial}{\partial r} \end{bmatrix}. \tag{8}$$

The stress–strain relations for layer i can be expressed as

$$\begin{Bmatrix} \sigma_{r,i} \\ \sigma_{\theta,i} \\ \tau_{rz,i} \end{Bmatrix} = \begin{bmatrix} C_{11,i} & C_{12,i} & 0 \\ C_{21,i} & C_{22,i} & 0 \\ 0 & 0 & C_{44,i} \end{bmatrix} \begin{Bmatrix} \varepsilon_{r,i} \\ \varepsilon_{\theta,i} \\ \gamma_{rz,i} \end{Bmatrix}, \tag{9a}$$

or

$$\boldsymbol{\sigma}_i = \boldsymbol{C}_i \varepsilon_i, \tag{9b}$$

where $\boldsymbol{C}_i$ is the elasticity matrix. For the isotropic material, the components of elasticity matrix are

$$C_{11,i} = C_{22,i} = \frac{E_i}{1 - v_i^2}, \quad C_{12,i} = C_{21,i} = \frac{v_i E_i}{1 - v_i^2}, \quad C_{44,i} = \kappa^2 \frac{E_i}{2(1 + v_i)}, \tag{10a-c}$$

here E_i is the Young's modulus, v_i is the Poisson ratio, and κ^2 is the shear correction factor. The shear correction is taken to be $\pi^2/12$ for layer 1 and layer 3 while to be 1 for layer 2. For the

isotropic linear viscoelastic material, assuming that viscoelastic material is almost incompressible and independent of frequency or temperature, the material constants are given by

$$E_i = E_v(1 + j\eta_v), \quad v_i = 0.5 - \delta, \tag{11a, b}$$

where η_v is the loss factor of the viscoelastic material, δ is assumed to be a small constant real value (e.g., $\delta = 0.001$) which is introduced to avoid material stiffness singularities, and $j = \sqrt{-1}$. The kinetic energy of the element e of layer i can be written as

$$T_i^e = \frac{1}{2}\oint_{V_e} \rho_i\{\dot{u}_i^2 + [(r + u_i)\Omega]^2 + \dot{w}_i^2\}\, dV, \tag{12a}$$

or in the matrix form

$$\begin{aligned} T_i^e = & \frac{1}{2}\oint_{V_e} \rho_i\big[\dot{\boldsymbol{u}}_i^{\mathrm{T}}\dot{\boldsymbol{u}}_i + \Omega^2(\boldsymbol{L}_3\boldsymbol{r}^{(0)})^{\mathrm{T}}(\boldsymbol{L}_3\boldsymbol{r}^{(0)}) + \Omega^2(\boldsymbol{L}_3\boldsymbol{u}_i)^{\mathrm{T}}(\boldsymbol{L}_3\boldsymbol{u}_i) \\ & + 2\Omega^2(\boldsymbol{L}_3\boldsymbol{u}_i)^{\mathrm{T}}(\boldsymbol{L}_3\boldsymbol{r}^{(0)})\big]\mathrm{d}V, \end{aligned} \tag{12b}$$

where the matrix $\boldsymbol{L}_3$ and the position vector $\boldsymbol{r}^{(0)}$ are

$$\boldsymbol{L}_3 = \begin{bmatrix} 1 & 0 \\ 0 & 0 \end{bmatrix}, \quad \boldsymbol{r}^{(0)} = \begin{Bmatrix} r \\ z \end{Bmatrix}, \tag{13a-b}$$

ρ_i is the mass density and $\oint_{V_e}$ represents a volume integral. The first term of kinetic energy in Eq. (12b) is due to vibratory motions of the plate. The second term is due to the rigid body motion and actually no contribution to the equations of motion. The third term is the supplementary strain energy due to displacement dependent centrifugal force. The fourth term is resulting from the initial in-plane stresses that are developed by the centrifugal force.

The strain energy of the annular element e of layer i is

$$U_i^e = \frac{1}{2}\oint_{V_e} \boldsymbol{\sigma}_i^{\mathrm{T}}\varepsilon_i\, dV + \oint_{V_e} \bar{\boldsymbol{\sigma}}_i^{e\mathrm{T}}\varepsilon_i^N\, \mathrm{d}V. \tag{14}$$

The second term in Eq. (14) is the additional strain energy induced by rotation. The rotation-induced stress vector $\bar{\boldsymbol{\sigma}}_i^e$ and the non-linear strain vector ε_i^N are

$$\bar{\boldsymbol{\sigma}}_i^e = \begin{Bmatrix} \bar{\sigma}_{r,i}^e & \bar{\sigma}_{\theta,i}^e & \bar{\tau}_{rz,i}^e \end{Bmatrix}^{\mathrm{T}} = \boldsymbol{C}_i(\mathscr{D}\boldsymbol{L}_{1,i}\boldsymbol{L}_2)\bar{\boldsymbol{U}}_i^e, \tag{15}$$

and

$$\varepsilon_i^N = \begin{Bmatrix} \dfrac{1}{2}\left(\dfrac{\partial u_i}{\partial r}\right)^2 + \dfrac{1}{2}\left(\dfrac{\partial w_i}{\partial r}\right)^2 \\ \dfrac{1}{2}\left(\dfrac{u_i}{r}\right)^2 \\ \dfrac{\partial u_i}{\partial r}\dfrac{\partial u_i}{\partial z} \end{Bmatrix}, \tag{16}$$

in which $\bar{\boldsymbol{U}}_i^e$ is the elemental equilibrium nodal displacement vector of the rotating annular element for layer i and is evaluated from the solutions of static problems. The details of this section are listed in Appendix A.

Substituting Eqs. (1),(3),(7) and (9) into Eqs. (12) and (14), the Hamilton's principle,

$$\delta\left[\int_t (T_i^e - U_i^e)\mathrm{d}t\right] = 0, \tag{17}$$

is used to derive element dynamic equilibrium equations. The element differential equations are expressed in matrix form as

$$\boldsymbol{M}_i^e \ddot{\boldsymbol{U}}_i^e + (\boldsymbol{K}_i^e + \boldsymbol{G}_i^e)\boldsymbol{U}_i^e = \boldsymbol{F}_i^e, \tag{18}$$

where the elemental mass matrix $\boldsymbol{M}_i^e$, elemental stiffness matrices $\boldsymbol{K}_i^e$ and $\boldsymbol{G}_i^e$, and elemental force vector $\boldsymbol{F}_i^e$ of layer i are

$$\boldsymbol{M}_i^e = \oint_{V_e} \left[\rho_i (\boldsymbol{L}_{1,i}\boldsymbol{L}_2)^{\mathrm{T}} (\boldsymbol{L}_{1,i}\boldsymbol{L}_2)\right] \mathrm{d}V, \tag{19}$$

$$\boldsymbol{K}_i^e = \oint_{V_e} \left[(\mathscr{D}\boldsymbol{L}_{1,i}\boldsymbol{L}_2)^{\mathrm{T}} \boldsymbol{C}_i^{\mathrm{T}} (\mathscr{D}\boldsymbol{L}_{1,i}\boldsymbol{L}_2) - \rho_i \Omega^2 (\boldsymbol{L}_3\boldsymbol{L}_{1,i}\boldsymbol{L}_2)^{\mathrm{T}} (\boldsymbol{L}_3\boldsymbol{L}_{1,i}\boldsymbol{L}_2)\right] \mathrm{d}V, \tag{20}$$

$$\begin{aligned} \boldsymbol{G}_i^e = 2 \oint_{V_e} & [(\mathscr{D}_1\boldsymbol{L}_4\boldsymbol{L}_{1,i}\boldsymbol{L}_2)^{\mathrm{T}} \hat{\boldsymbol{\sigma}}_i^e (\mathscr{D}_2\boldsymbol{L}_4\boldsymbol{L}_{1,i}\boldsymbol{L}_2) \\ & + (\mathscr{D}_1\boldsymbol{L}_5\boldsymbol{L}_{1,i}\boldsymbol{L}_2)^{\mathrm{T}} \hat{\boldsymbol{\sigma}}_i^e (\mathscr{D}_2\boldsymbol{L}_5\boldsymbol{L}_{1,i}\boldsymbol{L}_2) \\ & + \frac{1}{2}(\mathscr{D}_3\boldsymbol{L}_5\boldsymbol{L}_{1,i}\boldsymbol{L}_2)^{\mathrm{T}} \hat{\boldsymbol{\sigma}}_i^e (\mathscr{D}_3\boldsymbol{L}_5\boldsymbol{L}_{1,i}\boldsymbol{L}_2)\Big] \mathrm{d}V, \end{aligned} \tag{21}$$

$$\boldsymbol{F}_i^e = \oint_{V_e} \left[\rho_i \Omega^2 (\boldsymbol{L}_3\boldsymbol{L}_{1,i}\boldsymbol{L}_2)^{\mathrm{T}} (\boldsymbol{L}_3 \mathrm{r}^{(0)})\right] \mathrm{d}V, \tag{22}$$

and

$$\mathscr{D}_1 = \begin{Bmatrix} \frac{1}{2}\frac{\partial}{\partial r} \\ 0 \\ \frac{\partial}{\partial r} \end{Bmatrix}, \quad \mathscr{D}_2 = \begin{Bmatrix} \frac{\partial}{\partial r} \\ 0 \\ \frac{\partial}{\partial z} \end{Bmatrix}, \quad \mathscr{D}_3 = \begin{Bmatrix} 0 \\ \frac{1}{r} \\ 0 \end{Bmatrix}, \quad \hat{\boldsymbol{\sigma}}_i^e = \begin{bmatrix} \bar{\sigma}_{r,i}^e & 0 & 0 \\ 0 & \bar{\sigma}_{\theta,i}^e & 0 \\ 0 & 0 & \bar{\tau}_{rz,i}^e \end{bmatrix}, \tag{23a-d}$$

$$\boldsymbol{L}_4 = \begin{bmatrix} 1 & 0 \end{bmatrix}, \quad \boldsymbol{L}_5 = \begin{bmatrix} 0 & 1 \end{bmatrix}. \tag{23e-f}$$

The stiffness matrix $\boldsymbol{G}_i^e$ is usually called the geometric stiffness matrix that increases the plate stiffness.

Assembling the contribution of all elements, the global finite element equation can be obtained

$$\boldsymbol{M}\ddot{\boldsymbol{U}} + (\boldsymbol{K} + \boldsymbol{G})\boldsymbol{U} = \boldsymbol{F}, \tag{24}$$

where the global mass matrix $\boldsymbol{M}$, stiffness matrices $\boldsymbol{K}$ and $\boldsymbol{G}$, and force vector $\boldsymbol{F}$ are given by

$$\boldsymbol{M} = \sum_{i=1}^{3}\left(\sum_{e=1}^{N_i} \boldsymbol{T}_i^{e\mathrm{T}} \boldsymbol{M}_i^e \boldsymbol{T}_i^e\right), \tag{25}$$

$$\boldsymbol{K} = \sum_{i=1}^{3}\left(\sum_{e=1}^{N_i} \boldsymbol{T}_i^{e\mathrm{T}} \boldsymbol{K}_i^e \boldsymbol{T}_i^e\right), \tag{26}$$

$$\boldsymbol{G} = \sum_{i=1}^{3}\left(\sum_{e=1}^{N_i} \boldsymbol{T}_i^{e\mathrm{T}} \boldsymbol{G}_i^e \boldsymbol{T}_i^e\right), \tag{27}$$

$$\boldsymbol{F} = \sum_{i=1}^{3}\left(\sum_{e=1}^{N_i} \boldsymbol{T}_i^{e\mathrm{T}} \boldsymbol{F}_i^e\right), \tag{28}$$

N_i is the element number of layer i and the transformation matrix $\boldsymbol{T}_i^e$ must satisfy the following relation

$$\boldsymbol{U}_i^e = \boldsymbol{T}_i^e \boldsymbol{U}, \tag{29}$$

and $\boldsymbol{U}$ is the global nodal co-ordinate vector.

To study the free vibration of rotating annular plates, the forcing term in Eq. (24) is neglected and the eigenvalue equation can be obtained as follows

$$(\boldsymbol{K} + \boldsymbol{G})\boldsymbol{U} = \tilde{\lambda}\boldsymbol{M}\boldsymbol{U}, \tag{30}$$

where $\tilde{\lambda}$ is complex eigenvalue and can be found numerically. Both natural frequencies (ω) and modal loss factors (η) of the system are extracted in the following manner [6].

$$\omega = \sqrt{\mathrm{Re}(\tilde{\lambda})}, \quad \eta = \frac{\mathrm{Im}(\tilde{\lambda})}{\mathrm{Re}(\tilde{\lambda})}. \tag{31a-b}$$

3. Numerical results and discussion

The finite element method described in Section 2 is used to calculate the natural frequencies and modal loss factors of rotating annular plates with a constrained damping layer. To validate the proposed algorithm and calculations, comparisons between the present results and results of existing simplify model based on three-dimensional finite elements [14] are made first. The non-dimensional natural frequencies of the first and second axisymmetric transverse vibration modes of single material rotating thick annular plates are presented in Table 1. The material properties of plates are assumed to be linear elastic, homogenous and isotropic, however, the one-layered and the three-layered elements in the thickness direction are both used in computation of natural frequencies. The grids of the finite element meshes for the three-layered element in the thickness direction are equally spaced. The boundary conditions employed are clamped at inner radius

Table 1
Non-dimensional natural frequencies of the axisymmetric transverse vibration mode of the rotating annular plate made of single material ($a/b = 0.25$, $b/h = 10$, $v = 0.3$)

		$\bar{\omega}$					
	$N_r(N_z)$[a]	$\bar{\Omega} = 0$	$\bar{\Omega} = 2$	$\bar{\Omega} = 4$	$\bar{\Omega} = 8$	$\bar{\Omega} = 12$	$\bar{\Omega} = 16$
1st mode							
	4(1)	5.898	8.343	13.12	24.34	37.42	53.89
	8(1)	5.768	8.162	12.82	23.76	36.63	52.97
	16(1)	5.733	8.111	12.73	23.56	36.31	52.54
	32(1)	5.724	8.097	12.70	23.48	36.18	52.35
	4(3)	5.889	8.335	13.11	24.33	37.41	53.89
	8(3)	5.759	8.153	12.81	23.75	36.62	52.96
	16(3)	5.724	8.103	12.71	23.54	36.29	52.52
	32(3)	5.715	8.087	12.68	23.46	36.16	52.33
	Liu [14]	5.747	8.140	12.78	23.65	36.41	52.59
2nd mode							
	4(1)	36.84	40.17	48.91	75.36	109.5	153.1
	8(1)	34.16	37.51	46.24	72.36	106.0	149.4
	16(1)	33.49	36.85	45.56	71.49	104.8	147.9
	32(1)	33.31	36.66	45.35	71.21	104.4	147.3
	4(3)	36.62	39.97	48.76	75.28	109.4	153.1
	8(3)	33.94	37.32	46.09	72.28	106.0	149.4
	16(3)	33.27	36.65	45.40	71.40	104.8	147.9
	32(3)	33.09	36.46	45.20	71.11	104.4	147.3
	Liu [14]	33.49	36.93	45.80	72.06	105.7	149.1

[a] N_r: number of elements in the r direction, N_z: number of elements in the z direction.

$r = a$ and free at outer radius $r = b$. The rotational speed and natural frequency of the plate are non-dimensionalized as $\bar{\Omega} = \Omega b^2(\rho h/8D)^{1/2}$ and $\bar{\omega} = \omega b^2(\rho h/D)^{1/2}$, in which $D = Eh^3/\left[12\left(1-v^2\right)\right]$. As shown in Table 1, good convergences of the proposed formulations can be observed. It is also shown that the results agree well with those obtained by Liu et al. [14] for both one-layered element model and three-layered element model in various rotational speeds. Comparisons between published and proposed methods for the stationary clamped–free annular plate with fully constrained damping treatment are shown in Fig. 3. Numbers of elements in the r and z directions are chosen to be 16 and 3, respectively and the complex modulus representations of viscoelastic material are introduced into the middle layer. The present results and results of Ref. [15] are in agreement. The proposed algorithm and calculations about rotational and damping effects of the annular plate system are accuracy and reliable.

In the following studies, the material properties of damping layer and constraining layer are introduced into layer 2 and 3, respectively. The number of elements in the r direction is taken to be

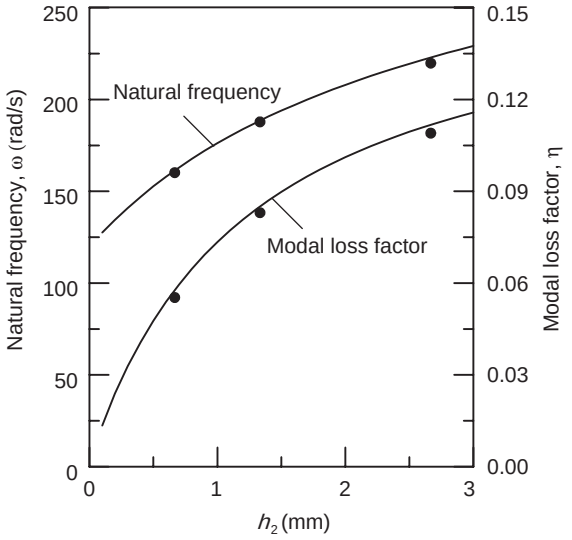

Fig. 3. Comparison between published and proposed methods for the stationary annular plate with fully constrained damping treatment. Key: ●●●, Ref. [15]; and ——, proposed. ($a = 60\,\text{mm}$, $b = 300\,\text{mm}$, $h_1 = h_3 = 0.667\,\text{mm}$, $\rho_1 = \rho_3 = 7850\,\text{kg/m}^3$, $\rho_2 = 1340\,\text{kg/m}^3$, $E_1 = E_3 = 2.1 \times 10^{11}\,\text{Pa}$, $E_2 = 2.3 \times 10^7 + j0.8 \times 10^7\,\text{Pa}$, $v_1 = v_3 = 0.29$, $v = 0.34$).

16. To simplify the calculation and further analysis, the following non-dimensional parameters are introduced:

$$\tilde{\xi} = \frac{a}{b}, \quad \tilde{a}' = \frac{a'}{b}, \quad \tilde{b}' = \frac{b'}{b}, \quad \tilde{b} = \frac{b}{h_1}, \quad \tilde{h}_2 = \frac{h_2}{h_1}, \quad \tilde{h}_3 = \frac{h_3}{h_1}, \quad \tilde{\rho}_2 = \frac{\rho_2}{\rho_1}, \tag{32a-g}$$

$$\tilde{\rho}_3 = \frac{\rho_3}{\rho_1}, \quad \tilde{E}_2 = \frac{\text{Re}(E_2)}{E_1}, \quad \tilde{E}_3 = \frac{E_3}{E_1}, \quad D_1 = \frac{E_1 h_1^3}{12(1 - v_1^2)}, \tag{32h-k}$$

$$\tilde{\Omega} = \Omega b^2 \sqrt{\frac{\rho_1 h_1}{8 D_1}}, \quad \tilde{\omega} = \omega b^2 \sqrt{\frac{\rho_1 h_1}{D_1}}. \tag{32l-m}$$

The non-dimensional frequencies and modal loss factors of rotating plates with fully constrained damping treatments are shown in Figs. 4(a) and (b). The effects of the modulus of viscoelastic layer $\tilde{E}_2$ in various rotational speeds $\tilde{\Omega} = 0$, 4 and 8 are studied. The boundary conditions of annular plates are clamped at inner radius and free at outer radius. A logarithmic scale of abscissa has been used to cover a wide range of $\tilde{E}_2$. It can be observed that the modulus $\tilde{E}_2$ has significant influences on both non-dimensional frequencies and modal loss factors. As $\tilde{E}_2$ increases, three distinct regions of frequencies for the first vibration mode are observed: compliant, transition, and stiff. The composite plates under larger rotational speed have higher non-dimensional frequency and smaller transition value of frequency from compliant region to stiff region. It is implied that the non-dimensional frequencies of the plate system under higher rotational speed are more insensitive as the modulus $\tilde{E}_2$ increases. As for the modal loss factors, it can be seen that the modal loss factors increase with increasing of $\tilde{E}_2$ at the lower value of $\tilde{E}_2$, but the phenomenon is reversed

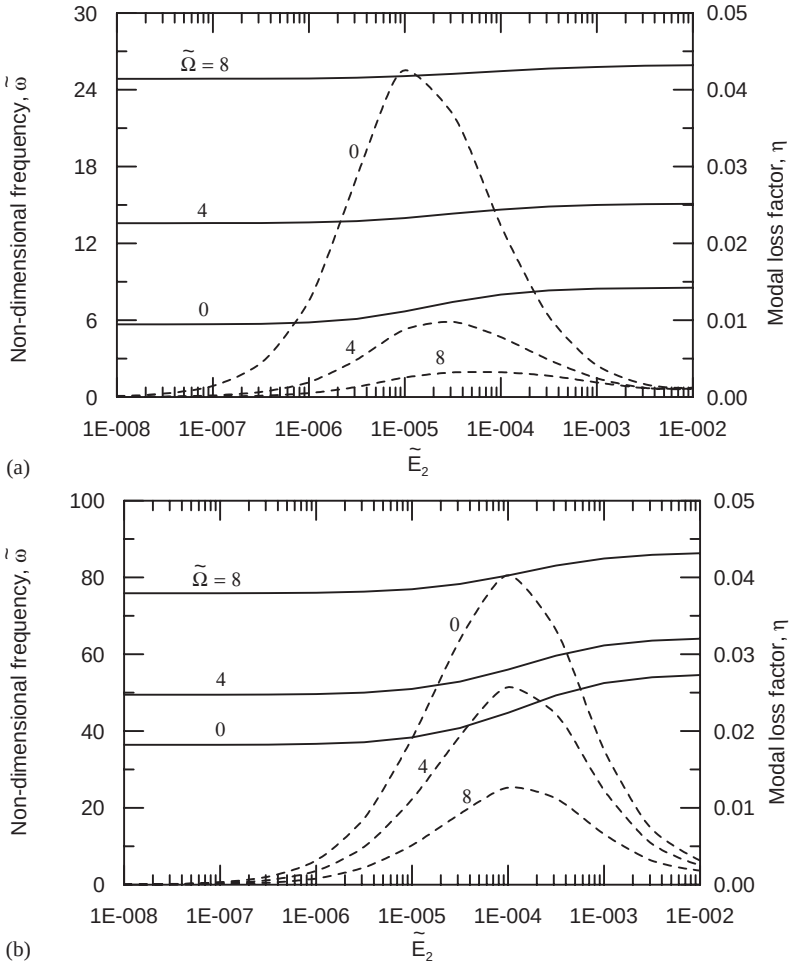

Fig. 4. Effects of $\tilde{E}_2$ on the non-dimensional frequencies and the modal loss factors of the rotating plate: (a) first mode; (b) second mode. Key: ——, non-dimensional frequency; - - - - -, modal loss factor. ($\tilde{\xi} = 0.3$, $\tilde{a}' = 0.3$, $\tilde{b}' = 1.0$, $\tilde{b} = 200$, $\tilde{h}_2 = \tilde{h}_3 = 0.2$, $\tilde{\rho}_2 = \tilde{\rho}_3 = 1$, $\tilde{E}_3 = 1$, $v_1 = v_3 = 0.3$,$\eta_v = 0.5$).

as $\tilde{E}_2$ increases above a certain value. Due to the effects of geometry stiffness matrix induced by centrifugal force, the plate system under larger rotational speed has smaller modal loss factor. The results for the second vibration mode are similar.

The effects of the modulus of the constraining layer $\tilde{E}_3$ on the non-dimensional frequencies and modal loss factors of the rotating composite plate are sketched in Figs. 5(a) and (b). It is shown that the modulus $\tilde{E}_3$ also has significant effects on the non-dimensional frequencies and modal loss factors. As expected, the stiffness of the plate increases with increasing of the modulus $\tilde{E}_3$ or the rotational speed $\tilde{\Omega}$. That is the non-dimensional frequencies increase as the modulus $\tilde{E}_3$ or the rotational speed $\tilde{\Omega}$ becomes larger. The effects of modulus $\tilde{E}_3$ on modal loss factor are similar to the effects of the modulus $\tilde{E}_2$. Also, it is seen that the non-dimensional frequencies increase rapidly when the modulus $\tilde{E}_3$ is greater than a certain value.

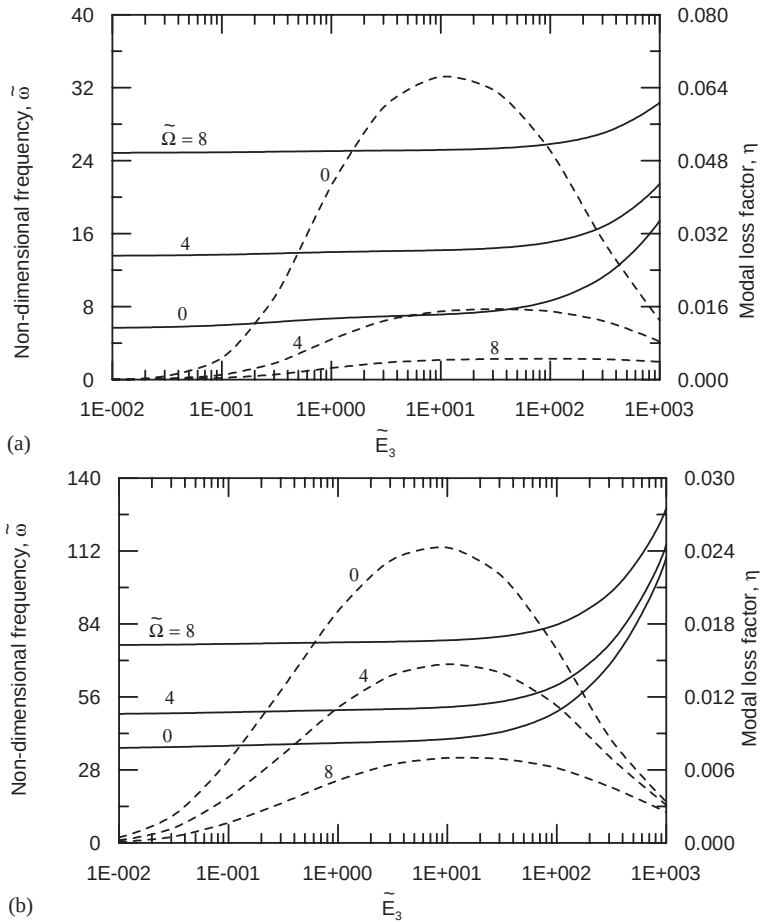

Fig. 5. Effects of $\tilde{E}_3$ on the non-dimensional frequencies and the modal loss factors of the rotating plate: (a) first mode; (b) second mode. Key: ——, non-dimensional frequency; - - - - -, modal loss factor. ($\tilde{\xi} = 0.3$, $\tilde{a}' = 0.3$, $\tilde{b}' = 1.0$, $\tilde{b} = 200$, $\tilde{h}_2 = \tilde{h}_3 = 0.2$, $\tilde{\rho}_2 = \tilde{\rho}_3 = 1$, $\tilde{E}_2 = 10^{-5}$, $v_1 = v_3 = 0.3$, $\eta_v = 0.5$).

The effects of the thickness of viscoelastic material layer and constraining layer on the non-dimensional frequencies and modal loss factors are now considered. The effects of $\tilde{h}_2$ are shown in Figs. 6(a) and (b). In practical applications the additional constraining and damping layers are always thinner than the host plate, and the non-dimensional thickness parameter $\tilde{h}_2$ is plotted in the range less than one. It can be seen that the frequencies decrease as $\tilde{h}_2$ increases. The reason is that the contribution of increasing thickness of the viscoelastic layer to the stiffness matrix of composite plates is more insignificant than those to the mass matrix of plates when the modulus $\tilde{E}_2$ is small. The frequencies increase with increasing rotational speed $\tilde{\Omega}$. For the first vibration mode, the modal loss factor of the stationary plate ($\tilde{\Omega} = 0$) always increases as $\tilde{h}_2$ increases can be found, but it is seen that the modal loss factors of the rotating plate are almost unchanged at higher value of $\tilde{h}_2$. It is indicated that the thicker viscoelastic layer is not provided the better damping of the rotating plate system. For the second vibration mode, it is found that the modal

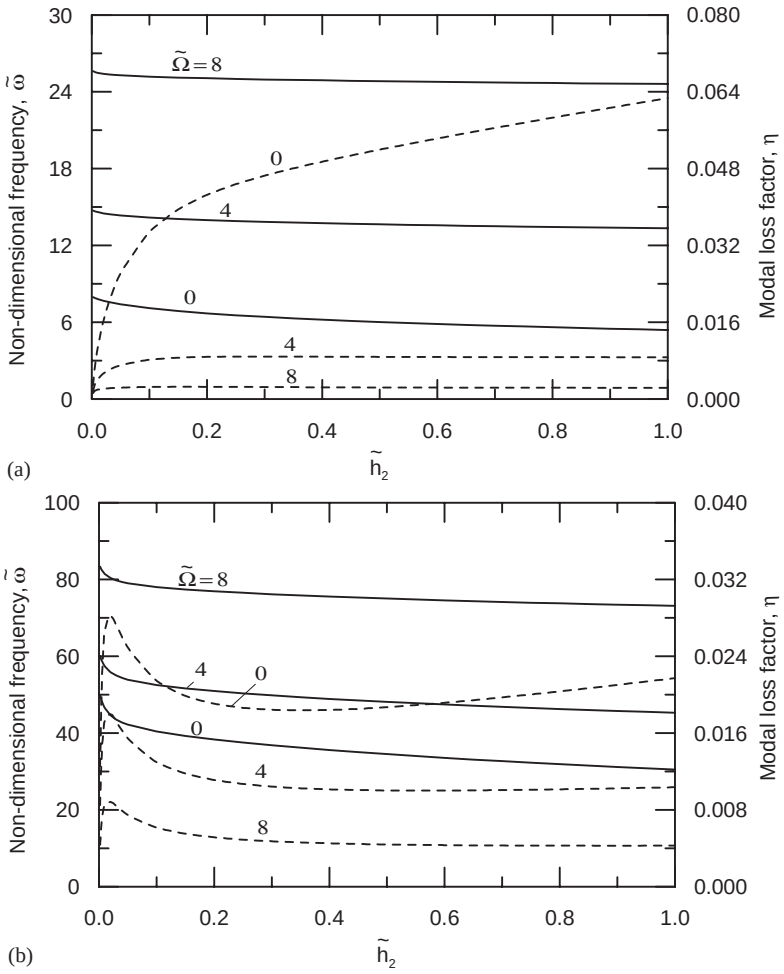

Fig. 6. Effects of $\tilde{h}_2$ on the non-dimensional frequencies and the modal loss factors of the rotating plate: (a) first mode; (b) second mode. Key: ——, non-dimensional frequency; ------, modal loss factor. ($\tilde{\xi} = 0.3$, $\tilde{\alpha}' = 0.3$, $\tilde{b}' = 1.0$, $\tilde{b} = 200$, $\tilde{h}_3 = 0.2$, $\tilde{\rho}_2 = \tilde{\rho}_3 = 1$, $\tilde{E}_2 = 10^{-5}$, $\tilde{E}_3 = 1$, $v_1 = v_3 = 0.3$, $\eta_v = 0.5$).

loss factors increase rapidly at the lower value of $\tilde{h}_2$, decrease when $\tilde{h}_2$ increases above a certain value, and then increase with increasing of $\tilde{h}_2$. The complex phenomenon is related to the stiffness of three layers and will be illustrated in Fig. 7.

Plots of the modal loss factors in various $\tilde{h}_2$ versus the modulus $\tilde{E}_2$ are shown in Fig. 7. It is shown that the higher-valued regions of modal loss factors are shifted to left as the thickness of viscoelastic layer $\tilde{h}_2$ become thinner. It is demonstrated that the thicker viscoelastic core layer is not provided better damping properties of the composite plate unless the suitable modulus and thickness of three layers are to be chosen. The effects of $\tilde{h}_3$ are plotted in Figs. 8(a) and (b). It is found that modal loss factors climb to a maximum value at an optimum value for the plate system under smaller rotational speed, but the maximum value of modal loss factor for the system under larger rotational speed is not seen when $\tilde{h}_3$ is less than one.

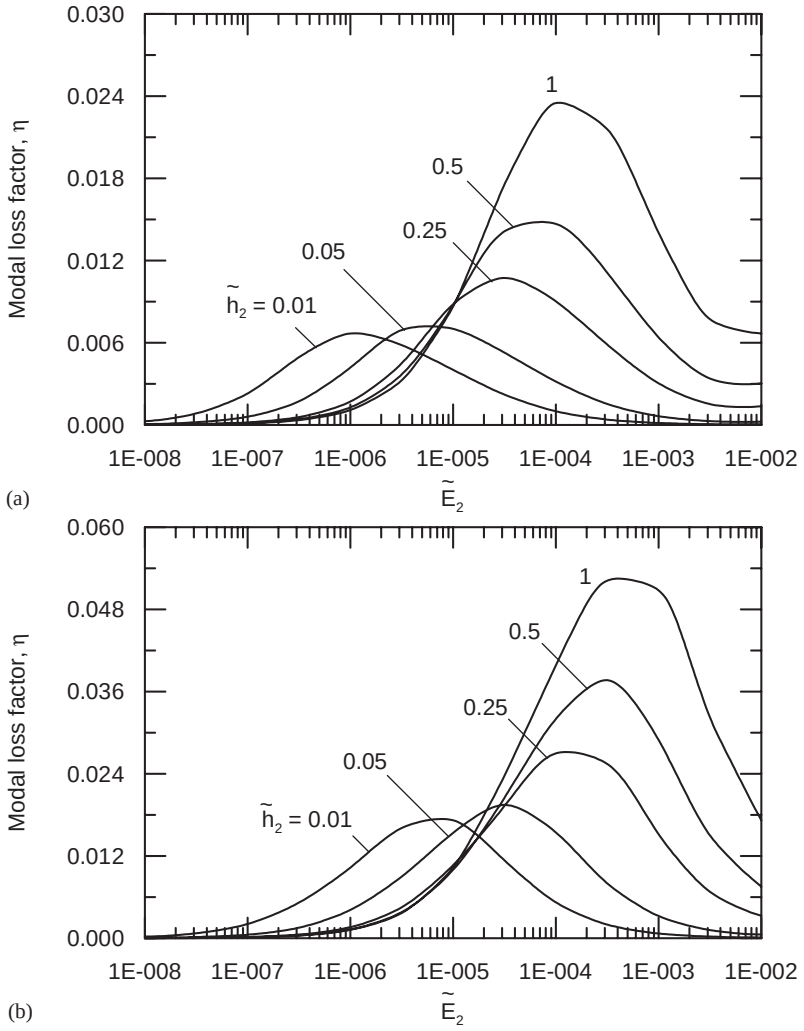

Fig. 7. The modal loss factors in various $\tilde{h}_2$ versus the modulus $\tilde{E}_2$: (a) first mode; (b) second mode. ($\tilde{\xi} = 0.3$, $\tilde{a}' = 0.3$, $\tilde{b}' = 1.0$, $\tilde{b} = 200$, $\tilde{h}_3 = 0.2$, $\tilde{\rho}_2 = \tilde{\rho}_3 = 1$, $\tilde{E}_3 = 1$, $\tilde{\Omega} = 4$, $v_1 = v_3 = 0.3$, $\eta_v = 0.5$).

The cases discussed above are rotating composite plates with full treatment clamped at inner radius of all three layers and free at the outer radius, as shown in Fig. 9(a). However, the systems with free-end treatment (Fig. 9(b)), simply supported-free boundary condition (Fig. 9(c)), and partial treatments (Figs. 9(e)–(g)) are also typical and practical cases in real situations. By taking advantage of discrete layer annular finite elements, these cases are all studied. The effects of $\tilde{\Omega}$ on the non-dimensional frequencies and modal loss factors of the rotating composite plate with different boundary conditions are shown in Figs. 10(a) and (b). The three types of boundary conditions, *CF*1, *CF*2, and *SF* are drawn in Figs. 9(a)–(c). It is shown that the frequencies increase rapidly with increasing of rotational speed and the modal loss factors are reversed. The order of the magnitude of frequencies for three different boundary conditions under the same

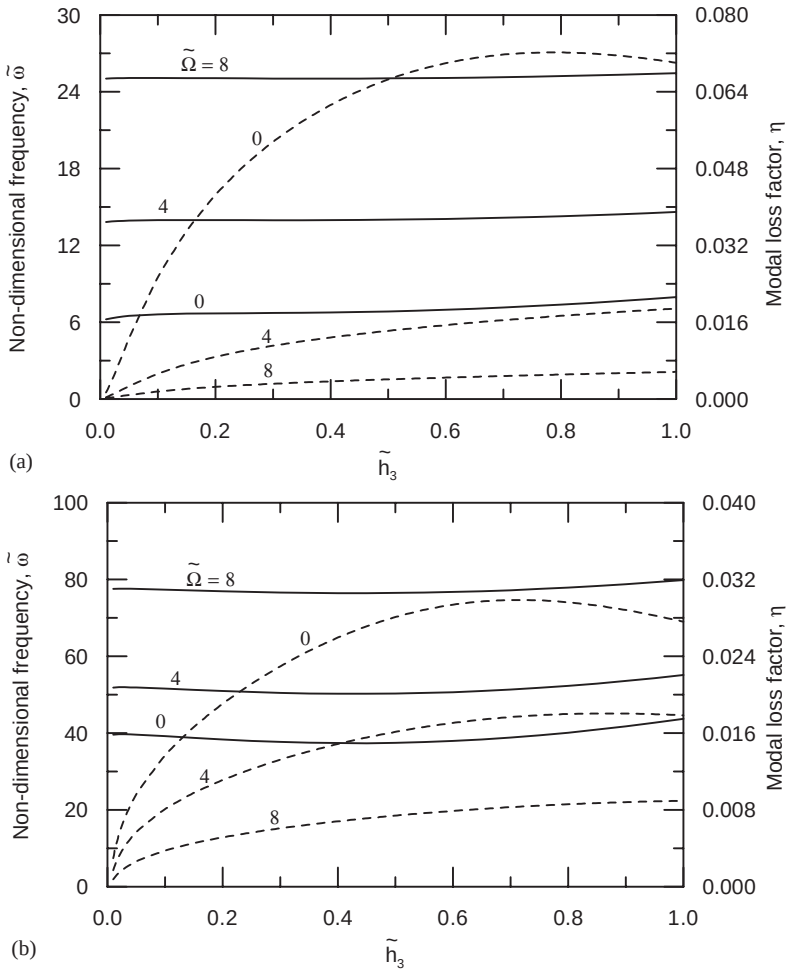

Fig. 8. Effects of $\tilde{h}_3$ on the non-dimensional frequencies and the modal loss factors of the rotating plate: (a) first mode; (b) second mode. Key: ——, non-dimensional frequency; - - - - -, modal loss factor. ($\tilde{\xi} = 0.3$, $\tilde{a}' = 0.3$, $\tilde{b}' = 1.0$, $\tilde{b} = 200$, $\tilde{h}_2 = 0.2$, $\tilde{\rho}_2 = \tilde{\rho}_3 = 1$, $\tilde{E}_2 = 10^{-5}$, $\tilde{E}_3 = 1$, $v_1 = v_3 = 0.3$,$\eta_v = 0.5$).

rotational speed is $CF1 > CF2 > SF$. For the modal loss factors, $SF > CF1 > CF2$ for the first vibration mode and $SF > CF1 \cong CF2$ for the second mode are seen. The damping layer undergoes larger shear deformation in the case with simply supported-free boundary condition during vibration.

The effects of $\tilde{\Omega}$ in various partial treatments are plotted in Figs. 11(a) and (b). The one-layered and three-layered elements are assembled to analyze the cases with partially constrained damping layer treatment. The three types of partial treatments are drawn in Figs. 9(e)–(g) and the plate with no treatment, Fig. 9(d), is also considered. It is seen that the modal loss factor for the first vibration mode of the plates with partial treatments $\tilde{b}' = 0.825$ and $\tilde{b}' = 1$ are almost the same as the rotational speed greater than some value. It is implied that the larger treatment in radial length is not provided the better damping. The reason is similar to the cases illustrated in Figs. 7(a) and (b).

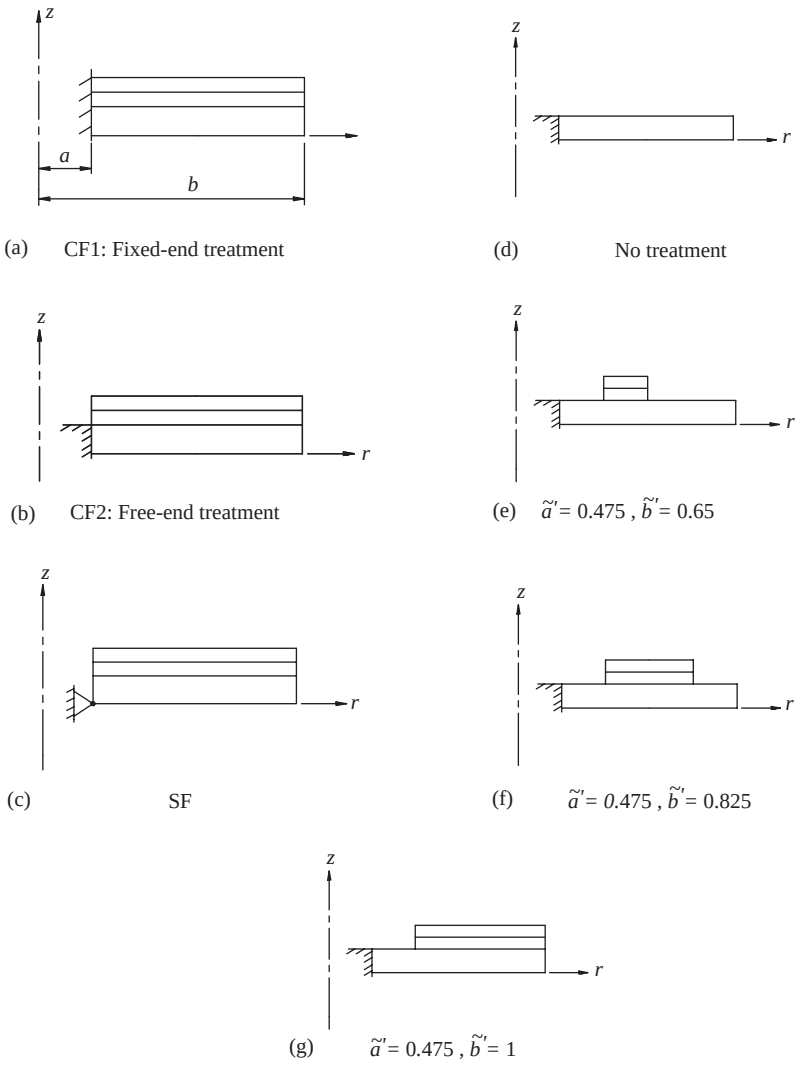

Fig. 9. Boundary conditions and partial treatments.

4. Conclusion

The paper studies the axisymmetric vibration and damping characteristics of the rotating annular plate with constrained damping layer treatment. The axisymmetric discrete layer annular finite elements are developed to analyze the rotating composite annular plate system in which the geometry stiffness matrix induced by rotation is evaluated from solutions of static problems. From the comparisons between the present results and published results of simplify model, it is shown that the algorithm and calculations made in the present paper are accuracy and reliable. Also, the discrete layer finite element method used is a quite feasible tool to discuss the cases with various types of partial treatments and boundary conditions.

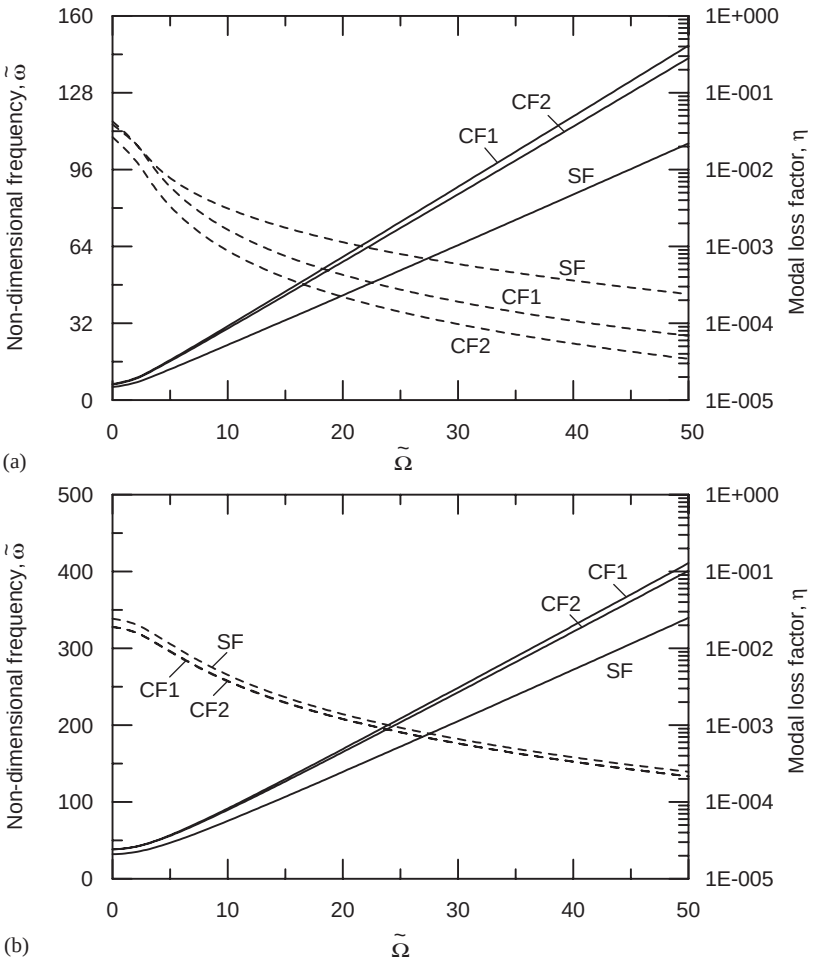

Fig. 10. Effects of $\tilde{\Omega}$ on the non-dimensional frequencies and modal loss factors of the rotating plate with different boundary conditions: (a) first mode; (b) second mode. Key: ——, non-dimensional frequency; - - - - -, modal loss factor. ($\tilde{\xi} = 0.3$, $\tilde{a}' = 0.3$, $\tilde{b}' = 1.0$, $\tilde{b} = 200$, $\tilde{h}_2 = \tilde{h}_3 = 0.2$, $\tilde{\rho}_2 = \tilde{\rho}_3 = 1$, $\tilde{E}_2 = 10^{-5}$, $\tilde{E}_3 = 1$, $v_1 = v_3 = 0.3$, $\eta_v = 0.5$).

Numerical results of example problems are seen that natural frequencies of the composite plate increase with increasing of rotational speed and modal loss factors are reversed. It is also shown that the stiffness and thickness of layers, boundary conditions, size of the treatment have significant influences on the natural frequencies and modal loss factors of the rotating composite plate. The thicker viscoelastic layer or the larger treatment size is not always provided better damping properties of the rotating composite plate system.

The axisymmetric discrete annular finite element used in the present paper can be extended to analyze a more general problem, e.g., the asymmetric vibration, but the degrees of freedom in the θ direction and the circumferential wave number must be considered. For the asymmetric vibration analysis of the rotating composite annular plate, the problem will not only become more complex in the computation but also involve the stability characteristics. And, the asymmetric vibration of rotating annular plate with constrained damping layer is one topic of further studies.

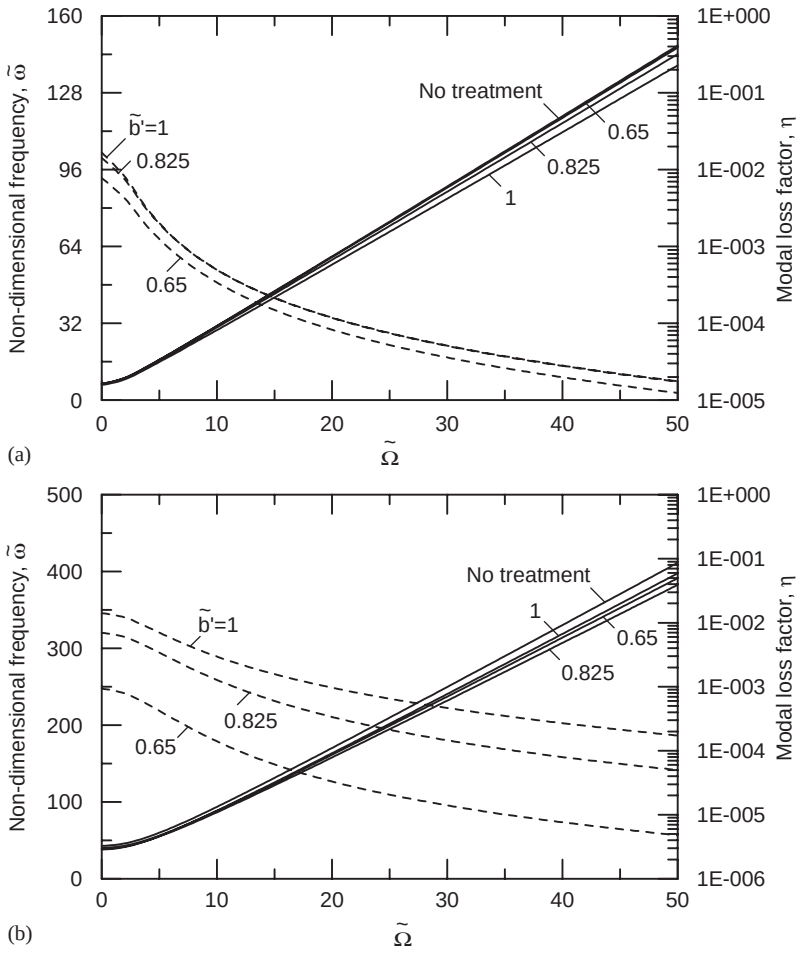

Fig. 11. Effects of $\tilde{\Omega}$ on the non-dimensional frequencies and the modal loss factors of the rotating plate with different partial treatments: (a) first mode; (b) second mode. Key: ——, non-dimensional frequency; - - - - -, modal loss factor. ($\tilde{\xi} = 0.3$, $\tilde{a}' = 0.475$, $\tilde{b} = 200$, $\tilde{h}_2 = \tilde{h}_3 = 0.2$, $\tilde{\rho}_2 = \tilde{\rho}_3 = 1$, $\tilde{E}_2 = 10^{-5}$, $\tilde{E}_3 = 1$, $v_1 = v_3 = 0.3$, $\eta_v = 0.5$).

Appendix A. Evaluation of elemental equilibrium nodal displacement vector

The elemental equilibrium nodal displacement vector $\bar{\boldsymbol{U}}_i^e$ is obtained from

$$\bar{\boldsymbol{U}}_i^e = \boldsymbol{T}_i^e \bar{\boldsymbol{U}}, \tag{A-1}$$

where $\boldsymbol{T}_i^e$ is the transformation matrix and $\bar{\boldsymbol{U}}$ is the global equilibrium nodal co-ordinate evaluated form the static problem of the whole system when the centrifugal force is applied,

$$\mathrm{Re}(\boldsymbol{K})\bar{\boldsymbol{U}} = \boldsymbol{F} \tag{A-2}$$

the stiffness matrix $\boldsymbol{K}$ and the centrifugal force vector $\boldsymbol{F}$ are the same as listed in Eqs. (26) and (28).

Appendix B. Nomenclature

A	inner radius of the host plate
a'	inner radius of the treatment
$\tilde{a}'$	a'/b, non-dimensional inner radius of the treatment
b	outer radius of the host plate
b'	outer radius of the treatment
$\tilde{b}$	b/h_1, outer radius to thickness ratio of the host plate
$\tilde{b}'$	b'/b, non-dimensional outer radius of the treatment
$C_{11,i}, C_{12,i}, C_{21,i}, C_{22,i}, C_{44,i},$	components of elasticity matrix for layer i
$\boldsymbol{C}_i$	elasticity matrix in layer i
D_1	$E_1 h_1^3/\left[12(1-v_1^2)\right]$, flexural rigidity of the host plate
$\mathscr{D}, \mathscr{D}_1, \mathscr{D}_2, \mathscr{D}_3$	differential operator matrix or vector
e	index for element
E_i	Young's modulus of layer i
E_v	storage modulus of the viscoelastic material
$\tilde{E}_2$	$\mathrm{Re}(E_2)/E_1$, non-dimensional stiffness of layer 2
$\tilde{E}_3$	E_3/E_1, non-dimensional stiffness of layer 3
$\boldsymbol{F}$	global force vector
$\boldsymbol{F}_i^e$	elemental force vector of layer i
$\boldsymbol{G}$	global geometry stiffness matrix
$\boldsymbol{G}_i^e$	elemental geometry stiffness matrix of layer i
h_i	thickness of layer i
$\tilde{h}_i$	h_i/h_1, non-dimensional thickness of layer i
i	index for layer, $i = 1, 2, 3$
j	$\sqrt{-1}$
$\boldsymbol{K}$	global stiffness matrix
$\boldsymbol{K}_i^e$	elemental stiffness matrix of layer i
$\boldsymbol{L}_{1,i}$	transverse thickness interpolation matrix for layer i
$\boldsymbol{L}_2$	interpolation matrix
$\boldsymbol{L}_3$	$\begin{bmatrix} 1 & 0 \\ 0 & 0 \end{bmatrix}$
$\boldsymbol{L}_4$	$\begin{bmatrix} 1 & 0 \end{bmatrix}$
$\boldsymbol{L}_5$	$\begin{bmatrix} 0 & 1 \end{bmatrix}$
$\boldsymbol{M}$	global mass matrix
$\boldsymbol{M}_i^e$	elemental mass matrix of layer i
n	number of internal nodal circles
$n_u^A, n_u^B, n_w^A, n_w^B, n_\Theta^A, n_\Theta^B$	components of the interpolation matrix $\boldsymbol{L}_2$
N_I	element number of layer i
r, z	cylindrical co-ordinate
r_i	inner radius of the annular element
r_o	outer radius of the annular element
$r^{(0)}$	position vector

t	time variable
$\boldsymbol{T}_i^e$	transformation matrix
T_i^e	kinetic energy of the element in layer i
$u_i, \quad w_i$	displacements in layer i
$\boldsymbol{u}_i$	displacement vector in layer i
$\boldsymbol{U}$	global nodal co-ordinate vector
$\boldsymbol{U}_i^e$	element nodal co-ordinate vector for layer i
U_i, U_{i+1}	displacements of the adjacent layer interfaces in the r-direction for layer i
$U_i^A, U_{i+1}^A, U_i^B, U_{i+1}^B$	element nodal displacements in the r-direction for layer i
U_i^e	strain energy of the element in layer i
$\bar{\boldsymbol{U}}_i^e$	elemental equilibrium nodal displacement vector
V_e	volume of the element
W	transverse displacement
W^A, W^B	element nodal displacements in the z-direction
δ	a small real constant
ε_i	strain vector in layer i
ε_i^N	non-linear strain vector
$\varepsilon_{r,i}, \varepsilon_{\theta,i}, \gamma_{rz,i}$	strains in layer i
η	modal loss factor of the composite plate
η_v	loss factor of the viscoelastic material
Θ^A, Θ^B	Elemental nodal rotation angles
κ^2	shear correction factor
$\tilde{\lambda}$	complex eigenvalue
v_i	Poisson's ratio of layer i
ξ	$(r - r_i)/(r_o - r_i)$
$\tilde{\xi}$	a/b , non-dimensional inner radius of the host plate
ρ_i	mass density of layer i
$\tilde{\rho}_i$	ρ_i/ρ_1 , non-dimensional mass density of layer i
$\boldsymbol{\sigma}_i$	stress vector in layer i
$\sigma_{r,i}, \sigma_{\theta,i}, \tau_{rz,i}$	stresses in layer i
$\bar{\boldsymbol{\sigma}}_i^e$	rotation-induced stress vector
ω	natural frequency
$\tilde{\omega}$	$\omega b^2\sqrt{\rho_1 h_1/D_1}$, non-dimensional frequency
Ω	rotational speed
$\tilde{\Omega}$	$\Omega b^2\sqrt{\rho_1 h_1/8D_1}$, non-dimensional rotational speed

References

[1] E.M. Kerwin Jr., Damping of flexural waves by a constrained viscoelastic layer, Journal of the Acoustical Society of America 31 (1959) 952–962.

[2] D. Ross, E.E. Ungar, E.M. Kerwin Jr., Damping of plate flexural vibrations by means of viscoelastic laminate, American Society of Mechanical Engineers, Structure Damping Section. 3 (1959) 49–88.

[3] R.A. DiTaranto, Theory of vibratory bending for elastic and viscoelastic layered finite-length beams, American Society of Mechanical Engineers Journal of Applied Mechanics 32 (1965) 881–886.
[4] D.J. Mead, The damping properties of elastically supported sandwich plates, Journal of Sound and Vibration 24 (1972) 275–295.
[5] Y.V.K.S. Rao, B.C. Nakra, Vibrations of unsymmetrical sandwich beams and plates with viscoelastic cores, Journal of Sound and Vibration 34 (1974) 309–326.
[6] R. Rikards, A. Chate, E. Barkanov, Finite element analysis of damping the vibrations of laminated composites, Computers and Structures 47 (1993) 1005–1015.
[7] P. Cupial, J. Niziol, Vibration and damping analysis of a three-layered composite plate with a viscoelastic mid-layer, Journal of Sound and Vibration 183 (1995) 99–114.
[8] J.A. Zapfe, G.A. Lesieutre, A discrete layer beam finite element for the dynamic analysis of composite sandwich beams with integral damping layers, Computers and Structures 70 (1999) 647–666.
[9] S.S. Rao, A.S. Prasad, Vibrations of annular plates including the effects of rotatory inertia and transverse shear deformation, Journal of Sound and Vibration 42 (1975) 305–324.
[10] T. Irie, G. Yamada, K. Takagi, Natural frequencies of thick annular plates, Journal of Applied Mechanics 49 (1982) 633–638.
[11] X. Wang, A.G. Striz, C.W. Bert, Free vibration analysis of annular plates by the DQ method, Journal of Sound and Vibration 164 (1993) 173–175.
[12] J. Kirkhope, G.J. Wilson, Vibration and stress analysis of thin rotating discs using annular finite elements, Journal of Sound and Vibration 44 (1976) 461–474.
[13] G.L. Nigh, M.D. Olson, Finite element analysis of rotating disks, Journal of Sound and Vibration 77 (1981) 61–78.
[14] C.F. Liu, J.F. Lee, Y.T. Lee, Axisymmetric vibration analysis of rotating annular plates by a 3D finite element, International Journal of Solids and Structures 37 (2000) 5813–5827.
[15] P.K. Roy, N. Ganesan, A vibration and damping analysis of circular plates with constrained damping layer treatment, Computers and Structures 49 (1993) 269–274.
[16] S.C. Yu, S.C. Huang, Vibration of a three-layered viscoelastic sandwich circular plate, International Journal of Mechanical Sciences 43 (2001) 2215–2236.
[17] S.L. Seubert, T.J. Anderson, R.E. Smelser, Passive damping of spinning disks, Journal of Vibration and Control 6 (2000) 715–725.